SOKOTO JOURNAL OF GEOGRAPHICAL STUDIES (SJGS) *E-ISSN: 3115-5812, PRINT ISSN: 3043-551X*

© DEPARTMENT OF GEOGRAPHY, SOKOTO STATE UNIVERSITY, SOKOTO

Volume 4, Issue 2, August 2026 Edition

HYDRO-CLIMATIC DYNAMICS OF NIGERIA'S RAINFOREST AGROECOLOGICAL ZONE

Adetayo, Adewale. O.[1], Eruola, Abayoymi. O.[2], [3]Dauda, Taofik. O.[3] & Balogun Ahmed. O.[4]

[1]Federal University Oye-Ekiti, Ekiti State, Nigeria
[2]Federal University of Agriculture Abeokuta, Ogun State, Nigeria
[3]Institute of Agricultural Research and Training, Obafemi Awolowo University, Ibadan, Nigeria
[4]Federal University of Technology, Akure, Nigeria

Corresponding Author's Email: wale_agromet@yahoo.com

Abstract **https://doi.org/10.65760/sjgs.v4.i2.8**

The intensification of the global hydrological cycle is expected to alter rainfall characteristics and atmospheric evaporative demand. This study analyzed a continuous 432-month (monthly) rainfall and evaporation record covering 1990–2025 to assess hydroclimatic variability, stationarity and extreme-rainfall frequency in Nigeria's rainforest agroecological zone. Descriptive statistics, Pearson correlation, Ordinary Least Squares (OLS) regression, Pettitt's change-point test, Augmented Dickey–Fuller (ADF) testing, Johansen cointegration analysis, the Aridity Index (AI), and extreme-event frequency analysis were applied. Rainfall and evaporation showed a strong inverse correlation ($r = -0.69$, $p < 0.001$). The Pettitt test detected no statistically significant abrupt change point ($p = 0.75$). The long-term mean Aridity Index was 22.42, indicating a very high moisture surplus under the classification adopted in this study. OLS regression indicated a marginal increase in annual rainfall of 1.62 mm yr−1 ($p = 0.1178$), while annual evaporation showed no significant trend (0.18 mm yr−1, $p = 0.46$). Extreme rainfall months, defined as months exceeding the 95th percentile threshold of 280.9 mm month−1, showed no clear increase in annual frequency over 1990–2025. The results indicate substantial seasonal and interannual variability in rainfall but comparatively low variability in evaporation. These findings provide a baseline for evaluating hydroclimatic variability and water-resource management in a humid rainforest environment.

Keywords: *Stationarity, Hyper-humid, Rainfall Variability, Evaporation, Aridity Index, Extreme Rainfall.*

Introduction

The intensification of the global hydrological cycle is one of the important consequences of anthropogenic climate warming. As atmospheric moisture-holding capacity increases with temperature, changes in precipitation characteristics and atmospheric evaporative demand are expected across many regions (Gleeson *et al*., 2020; IPCC, 2023). While much of the literature emphasizes water-limited environments where increasing aridity poses risks to food and water security, humid and energy-limited environments also require investigation because their hydrological responses are constrained by the availability of energy rather than water (Han *et al*., 2020; Greve *et al*., 2021). The concept of hydrological non-stationarity has therefore generated continuing debate about whether historical observations remain adequate baselines for understanding future water risks (Brunner *et al*., 2023; Serinaldi & Kilsby, 2021).

Catchments can broadly be characterized as water-limited, where evapotranspiration is constrained by available moisture, or energy-limited, where water is abundant and evapotranspiration is

constrained more strongly by available energy (Gudmundsson *et al.*, 2021; Moussa & Lhomme, 2023). In humid environments, persistent cloud cover, high atmospheric humidity and seasonal rainfall can moderate evaporative losses and produce strong coupling between rainfall seasonality and atmospheric water demand (Wang *et al*., 2022). The so-called evaporation paradox, in which evaporation or evaporative demand may remain stable or decline in some regions despite warming, has consequently become an important research issue (McVicar *et al*., 2022).

Determining whether humid basins are undergoing systematic hydroclimatic change or remaining within a relatively stable statistical envelope is important for water-resource planning. However, an important gap remains in integrated, long-term assessments of Nigeria's rainforest agroecological zone that simultaneously examine rainfall, evaporation, moisture-regime characteristics, extreme-rainfall frequency and statistical stationarity using a continuous monthly record. Existing studies have often focused on individual rainfall characteristics, broader regional patterns or shorter periods, making it difficult to evaluate how rainfall and evaporation jointly behave over several decades. Addressing this gap is particularly relevant because southern Nigeria has a strongly seasonal rainfall regime, including the characteristic August break and a second rainfall maximum later in the wet season (Chineke *et al*., 2020).

This study uses a continuous monthly record of rainfall and evaporation from 1990–2025 (432 monthly observations) to characterize the hydroclimatic dynamics of Nigeria's rainforest agroecological zone. Specifically, the study examines (i) long-term trends and stationarity in rainfall and evaporation, (ii) the moisture regime using the Aridity Index, (iii) the relationship between rainfall and evaporation, and (iv) the temporal frequency of extreme rainfall months. The study provides a baseline for understanding hydroclimatic variability and for supporting climate-sensitive water-resource planning in humid environments.

Methodology

Study Area

Nigeria's rainforest agroecological zone covers about 115,000 km² and is characterized by a humid tropical climate with distinct wet and dry seasons. Rainfall in southern Nigeria commonly exhibits a bimodal seasonal pattern, with a first maximum around June–July, an August break, and a second maximum around September (Chineke et al., 2010). The Nigerian Meteorological Agency (NiMet) also provides seasonal climate information for southern Nigeria, including rainfall onset, cessation, length of season and rainfall amount, reflecting marked spatial and seasonal variability in the region (NiMet, 2025). Mean monthly temperatures are generally high throughout the year, with relatively small annual fluctuations. The mean monthly maximum temperature ranges from about 28°C to 35°C, while mean monthly minimum temperature ranges from approximately 22.6°C to 26.7°C. Relative humidity is high during the rainy season and lower during the drier months. The geomorphology and physiography comprise relatively flat to gently undulating lowlands developed mainly on sedimentary rocks and littoral deposits, including sandstone and shale. These climatic and physiographic characteristics provide a suitable setting for examining rainfall–evaporation relationships and hydroclimatic variability.

https://doi.org/10.65760/sjgs.v4.i2.8

© DEPARTMENT OF GEOGRAPHY, SOKOTO STATE UNIVERSITY, SOKOTO

Volume 4, Issue 2, August 2026 Edition

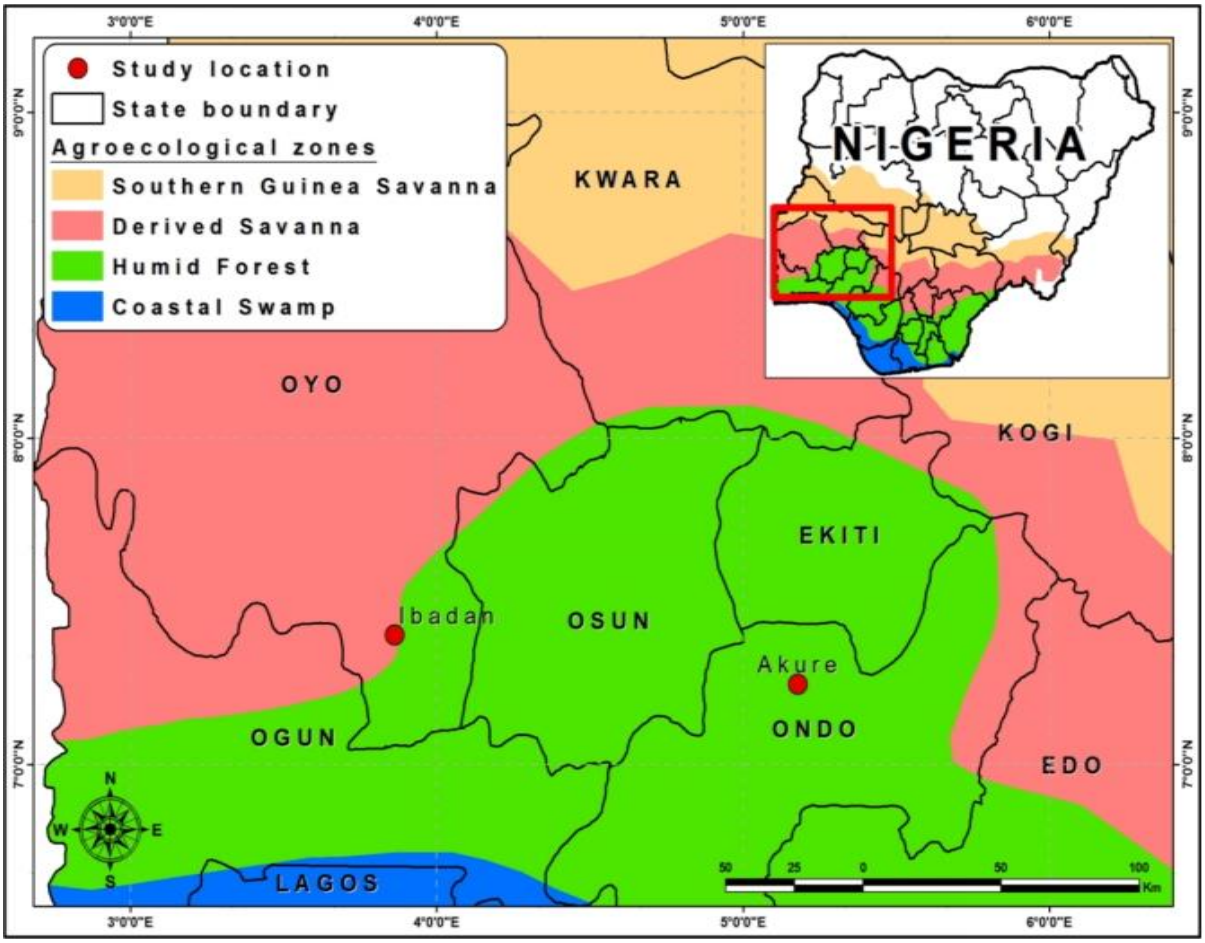


Figure 1: Study Area

Data Collection, Pre-processing and Quality Assurance

Monthly rainfall and evaporation data covering January 1990–December 2025 were obtained from the Nigerian Meteorological Agency (NiMet), Abuja, Nigeria. The dataset therefore contains 432 monthly observations (36 complete calendar years). The period 1990–2025 was selected because it provides a continuous multi-decadal record long enough to characterize seasonal and interannual variability, evaluate long-term trends and statistical stationarity, and quantify the frequency of extreme monthly rainfall events across several decades. The data were screened for missing or inconsistent observations before analysis; the study used the continuous monthly record for subsequent statistical analyses.

Hydro-climatic Characterization (Aridity Index)

To quantify the moisture regime of the study area, the Aridity Index (AI) was calculated as the ratio of precipitation to potential evaporation (AI = P/E). Annual AI values were calculated from the corresponding annual rainfall and evaporation totals to assess interannual variability in the moisture regime. The study adopted the following descriptive classification for the observed moisture surplus: Hyper-humid, $P/E > 2.0$; Humid, $1.5 < P/E \leq 2.0$; and Sub-humid, $1.0 < P/E \leq 1.5$. These thresholds are used here as the study-specific classification described in the original analysis and should not be interpreted as the standard UNEP aridity classification.

https://doi.org/10.65760/sjgs.v4.i2.8

Trend Analysis and Stationarity Testing

Descriptive statistics were first calculated for monthly rainfall and evaporation, including the mean, standard deviation, minimum, maximum, coefficient of variation and Pearson correlation coefficient. Long-term trajectories in annual rainfall and evaporation were then quantified using Ordinary Least Squares (OLS) linear regression. The regression slope (β) represents the estimated annual rate of change in mm yr−1, and significance was evaluated using a two-tailed Student's t-test at $\alpha = 0.05$. Pettitt's non-parametric change-point test was used to examine whether a statistically significant abrupt shift occurred in the series. The Augmented Dickey–Fuller (ADF) test was applied to the rainfall and evaporation series to assess unit-root stationarity; where the level series was non-stationary, first differencing was applied and the test repeated. Johansen trace and maximum-eigenvalue tests were used to assess long-run cointegration between rainfall and evaporation.

Pluviometric Volatility and Extreme Event Analysis

To evaluate extreme monthly rainfall, the 95th percentile of the complete 432-month rainfall distribution was calculated. The resulting threshold of 280.9 mm month−1 was used to classify months with rainfall above this value as extreme rainfall months. The threshold was applied consistently across the study period to permit comparison of event frequency through time.

Extreme-event frequency was summarized using the following procedures:

1. Binary categorization: each month exceeding the 95th percentile threshold (280.9 mm month−1) was classified as an extreme rainfall month.
2. Decadal aggregation: extreme events were grouped into 1990–1999, 2000–2009, 2010–2019 and 2020–2025 to identify temporal differences in frequency.
3. Frequency trend analysis: the annual number of extreme rainfall months was examined to determine whether their frequency increased or decreased through 1990–2025.

Extreme Value Analysis (EVA) and Stationarity of Volatility

Extreme-event frequency analysis was used to evaluate whether the observed frequency of high-rainfall months changed over the study period.

1. Threshold selection: extreme rainfall months were defined as observations exceeding the 95th percentile of the complete 432-month rainfall distribution.
2. Annual frequency series: the number of extreme rainfall months in each calendar year was counted and treated as a time series for assessing temporal variability.
3. Unit-root testing: the Augmented Dickey–Fuller (ADF) test was applied to the rainfall and evaporation series at level and, where necessary, after first differencing to determine the order at which the series became stationary.

Results

The descriptive statistics showed a seasonal hydrological regime with a substantial rainfall surplus over evaporation. Mean monthly rainfall was 100.49 mm with a standard deviation of 103.37 mm, while mean monthly evaporation was 4.80 mm and the maximum monthly evaporation was 8.8 mm. The standard deviation of rainfall was slightly greater than its mean, indicating pronounced month-

https://doi.org/10.65760/sjgs.v4.i2.8

to-month variability associated with the seasonal rainfall regime. Rainfall and evaporation were strongly negatively correlated ($r = -0.69$, $p < 0.001$), indicating that months with high rainfall generally coincided with lower evaporation in the observed record. The ADF results in Table 1 show that both series became stationary after first differencing, with ADF statistics of −29.73 for evaporation and −33.76 for rainfall, both more negative than the reported critical values at the 1%, 5% and 10% levels.

Table 1. Augmented Dickey–Fuller (ADF) unit-root test results for first-differenced rainfall and evaporation.

Variable	ADF Statistic	1% Critical Value	5% Critical Value	10% Critical Value
D(EVAPORATION)	-29.73	-3.98	-3.421	-3.133
D(RAINFALL)	-33.76	-3.98	-3.421	-3.133

The Johansen cointegration results (Table 2) indicate a statistically significant long-run relationship between rainfall and evaporation. The trace statistic for the null hypothesis of no cointegrating relationship was 202.45, compared with a 5% critical value of 15.495, while the maximum-eigenvalue statistic was 155.02 compared with a 5% critical value of 14.265. These results indicate that, although rainfall and evaporation fluctuate substantially from month to month, the two series exhibit a statistically detectable long-run association over 1990–2025.

Table 2. Johansen cointegration test results for rainfall and evaporation.

	Hypothesized No. of CE(s)	**Eigenvalue**	**Trace Statistic**	**5% Critical Value**
Trace Test	None	0.3044	202.45	15.495
	At most 1	0.1051	47.436	3.8415
	Hypothesized No. of CE(s)	Eigenvalue	Max-Eigen Statistic	5% Critical Value
Maximum Eigen Value	None	0.3044	155.02	14.265
	At most 1	0.1051	47.436	3.8415

Figure 2 presents the monthly rainfall, evaporation and hydrological balance (P − E) over the study record. Rainfall is highly seasonal, with repeated peaks above 250 mm month−1 and occasional values above 300 mm month−1, whereas evaporation remains comparatively low and stable. The P − E series is positive for most months, indicating a persistent monthly rainfall surplus over

https://doi.org/10.65760/sjgs.v4.i2.8

evaporation. Short periods of near-zero or slightly negative balance occur during the driest months, but these are small relative to the positive balances recorded during the rainy season.

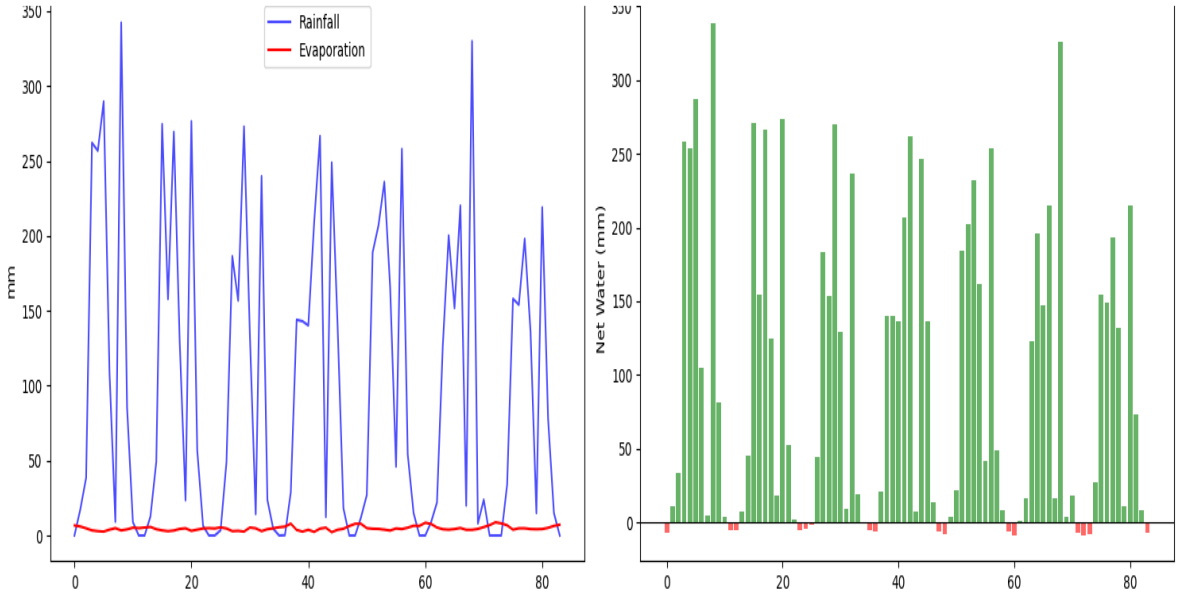


Figure 2: Monthly rainfall and evaporation and hydrological balance (P − E), 1990–2025.

Figure 3 shows the monthly rainfall and evaporation series from 1990–2025. Rainfall displays pronounced seasonal and interannual variability, with frequent monthly peaks between 200 and 400 mm. Evaporation remains comparatively stable, generally within a much smaller range. A particularly large rainfall event occurred around 2018–2019, when monthly rainfall approached 500 mm. Other notable high-rainfall peaks occurred around 1994, 2007 and 2024. The contrast between the two series highlights the much greater temporal variability of rainfall relative to evaporation in the study area.

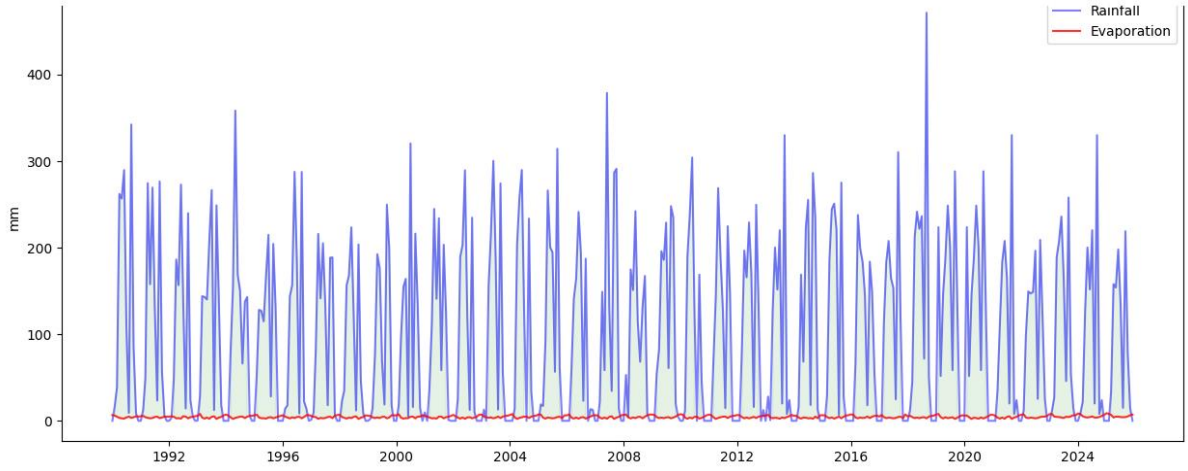


Figure 3: Monthly rainfall and evaporation fluxes, 1990–2025.

https://doi.org/10.65760/sjgs.v4.i2.8

Figure 4 presents the temporal distribution and decadal frequency of extreme rainfall months defined by the 95th percentile threshold of 280.9 mm month−1. Extreme events occurred throughout the study period but were not evenly distributed. The most pronounced event occurred around 2018–2019, when monthly rainfall approached 500 mm. The 2000–2009 period recorded the highest number of extreme months (8), followed by 2010–2019 (6), 1990–1999 (5) and 2020–2025 (3). Because the final interval covers only six years, its lower count should not be interpreted directly as evidence of a declining long-term frequency without adjustment for the unequal interval lengths.

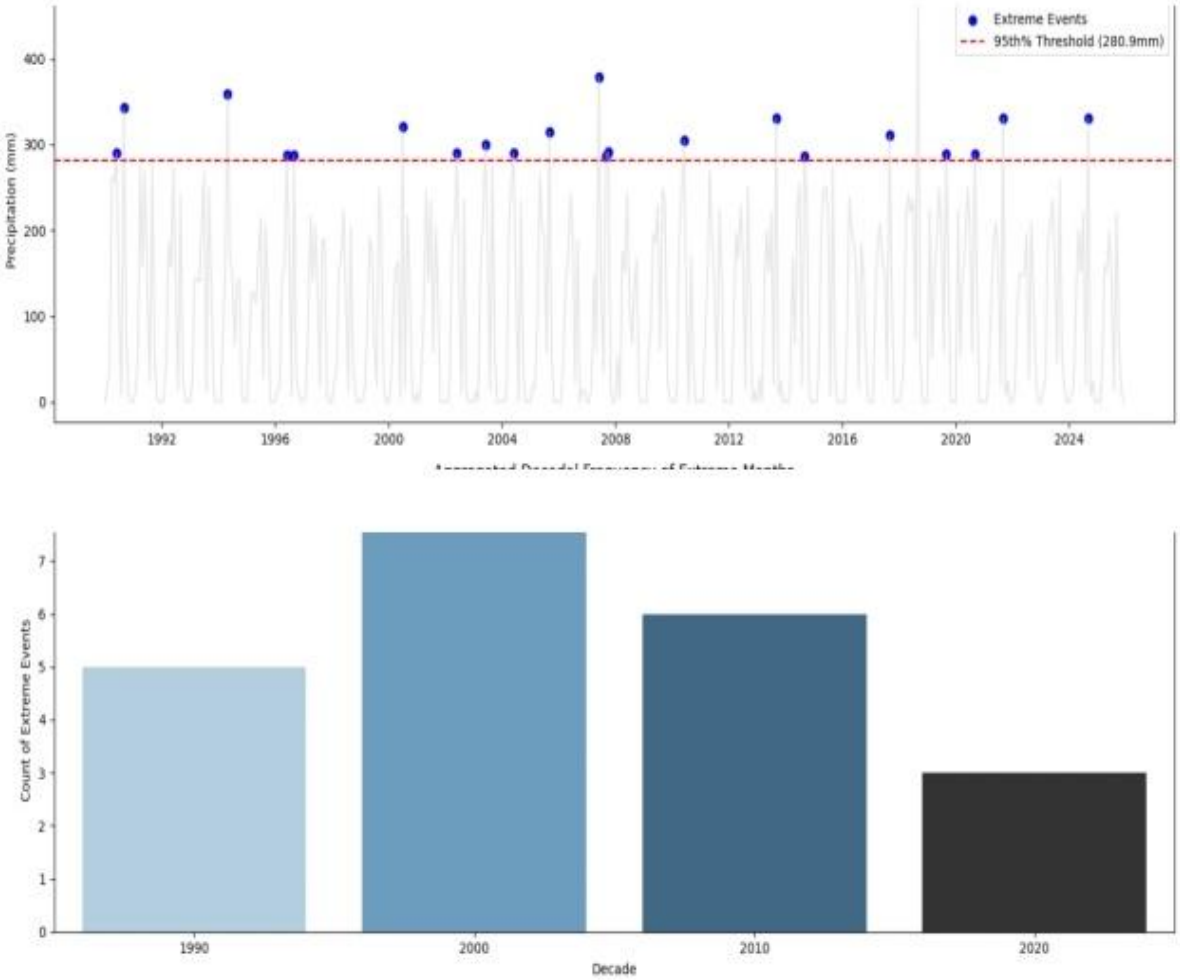


Figure 4: Chronological distribution and decadal frequency of extreme rainfall months (>280.9 mm month−1), 1990–2025.

Figure 5 summarizes the annual Aridity Index, the monthly rainfall–evaporation surplus and the decadal count of extreme rainfall months. Annual AI values were consistently far above the adopted humid threshold, confirming a strong moisture surplus throughout 1990–2025. The highest AI values occurred around 2018–2020, coinciding with relatively high rainfall totals, while lower values were observed toward 2024–2025. The monthly surplus panel shows that rainfall generally exceeded evaporation, particularly during the wet season. The decadal frequency panel confirms that 2000–

https://doi.org/10.65760/sjgs.v4.i2.8

2009 had the largest number of extreme rainfall months, whereas 2020–2025 recorded fewer events over a shorter interval.



Figure 5: Annual Aridity Index, monthly rainfall–evaporation surplus, and decadal frequency of extreme rainfall months, 1990–2025.

The annual rainfall and evaporation totals for 1990–2025 are presented in Figure 6. Annual rainfall shows substantial interannual variability, with most annual totals between approximately 1,000 and 1,400 mm and a wetter cluster around 2018–2020 when totals approached or exceeded 1,600 mm. The fitted rainfall line has a small positive slope, consistent with the OLS estimate of 1.62 mm yr−1, but the trend is not statistically significant ($p = 0.1178$). Annual evaporation remains comparatively stable, with values clustered near 50–60 mm yr−1; its fitted trend is also not statistically significant (0.18 mm yr−1, $p = 0.46$). The confidence band around the rainfall regression reflects uncertainty around the estimated mean trend and should not be interpreted as a forecast interval.

https://doi.org/10.65760/sjgs.v4.i2.8

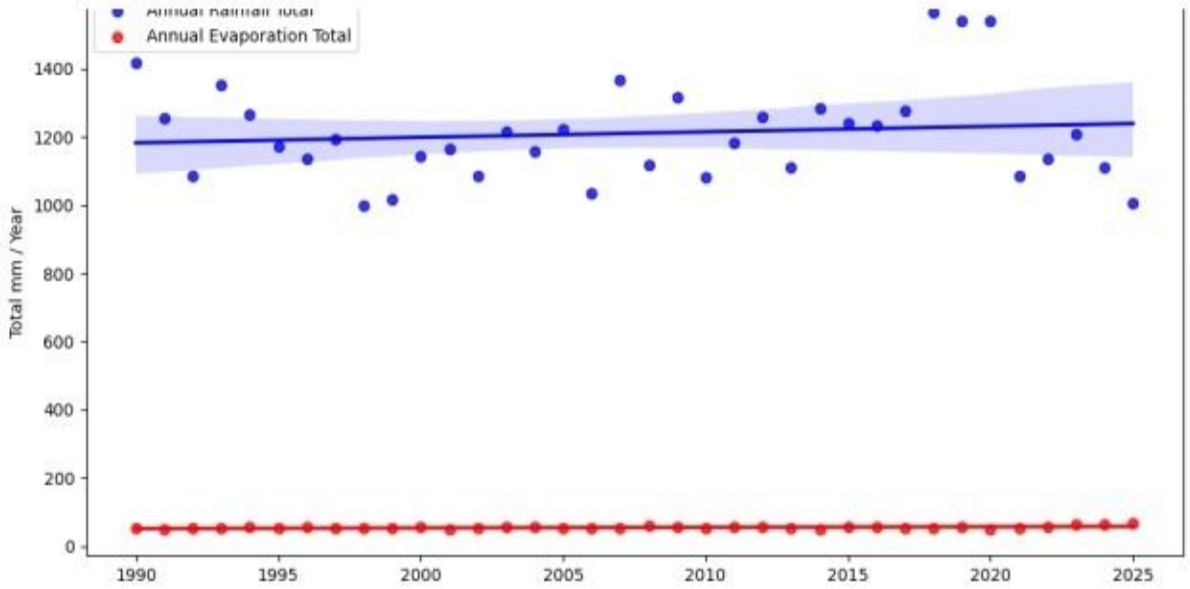


Figure 6: Annual rainfall and evaporation totals, 1990–2025.

Figure 7 presents mean monthly rainfall and evaporation for 1990–2025 and highlights the seasonal cycle. Rainfall follows a bimodal pattern, increasing from the early rainy season to a first peak around June, declining markedly in August, and rising again to a second peak around September before decreasing rapidly in October. November to January are the driest months, while February and March represent the transition into the main rainy season. Evaporation remains much lower than rainfall throughout the year, although it varies seasonally. The figure therefore confirms that the large rainfall surplus is concentrated in the wet season and that the August break is evident in the long-term monthly climatology.

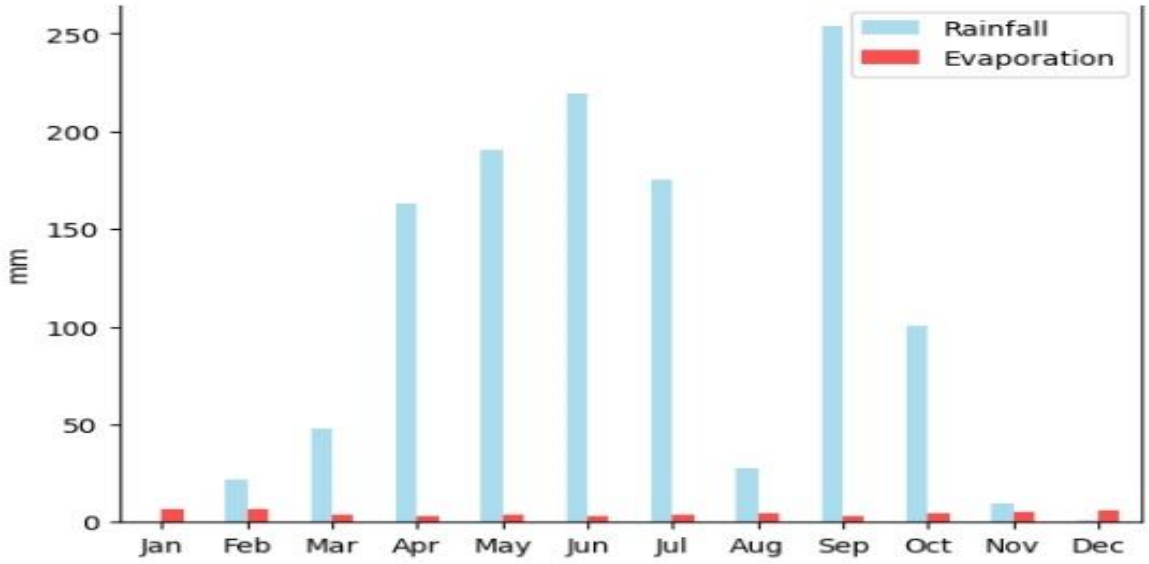


Figure 7: Mean monthly rainfall and evaporation, 1990–2025.

https://doi.org/10.65760/sjgs.v4.i2.8

Figure 8 compares mean monthly rainfall and evaporation across the periods 1990–1999, 2000–2009, 2010–2019 and 2020–2025. Mean monthly rainfall was approximately 99 mm in the 1990s and 2000s, increased to about 106 mm in the 2010s, and declined toward approximately 100 mm in 2020–2025. Mean evaporation remained close to 5 mm month−1 across the four periods. The comparison therefore indicates decadal variability in rainfall totals without a corresponding large change in mean evaporation.

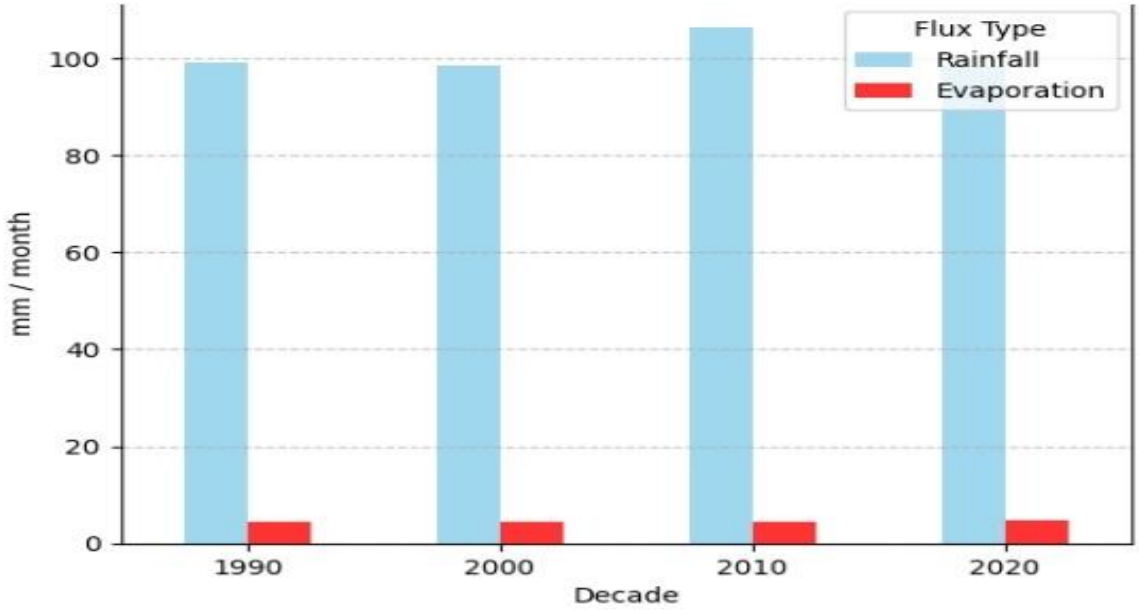


Figure 8: Decadal mean rainfall and evaporation, 1990–2025.

Discussion

The strong negative correlation between rainfall and evaporation indicates that the two variables vary in opposite directions at the monthly scale. Such an inverse association is consistent with the physical idea that wetter periods are often associated with greater cloudiness and reduced available energy for evaporation, although correlation alone does not establish the underlying mechanism (Pokhrel et al., 2021; McVicar et al., 2022). The persistent positive P − E balance and the high Aridity Index indicate that rainfall substantially exceeds the observed evaporation throughout most of the record. This moisture surplus is an important characteristic of the rainforest agroecological environment and provides a useful baseline for assessing future changes in rainfall and evaporative demand.

The mean Aridity Index of 22.42 places the study area well within the very humid end of the study-specific classification adopted here. Within a Budyko framework, such a high precipitation-to-evaporation ratio is consistent with a moisture-abundant environment in which evaporative losses are more likely to be constrained by available energy than by water supply (Han et al., 2023; Han et al., 2020). However, the present dataset does not include direct measurements of net radiation, soil moisture or actual evapotranspiration; therefore, the inferred energy limitation should be regarded as a plausible hydroclimatic interpretation rather than a directly measured mechanism. The absence of a significant rainfall trend ($p = 0.1178$) and the non-significant evaporation trend ($p = 0.46$) further

https://doi.org/10.65760/sjgs.v4.i2.8

indicate that no statistically significant monotonic change was detected in either annual series over 1990–2025.

The negative or near-zero monthly water balances observed during some dry-season months, including the anomaly around February 2024, indicate short-lived periods of reduced moisture availability. These observations should not, however, be classified as flash droughts solely from rainfall and evaporation data. A formal flash-drought diagnosis generally requires evidence of rapid soil-moisture depletion and/or increasing evaporative demand over a defined period (Blum *et al*., 2020). The present study therefore interprets the February 2024 event as a short-duration moisture deficit rather than a confirmed flash drought. This distinction is important because the annual water balance remains strongly positive even when individual dry-season months experience temporary deficits.

Conclusions and Recommendations

Basin remains a resilient water tower where hydrological processes are currently absorbed by high drainage capacity without a shift in catastrophic frequency. Results from this study demonstrated that while global climate forcing is ubiquitous, its expression at the catchment scale is highly filtered by local energy-limited constraints. The frequency of extreme events over three and a half decades suggests that the probability distribution of rainfall in this basin remains stationary. This challenges the universal application of non-stationary models and suggests that certain high-surplus catchments may serve as geophysical buffers against global climatic volatility. The decoupling of rainfall and evaporation confirms that the local atmosphere is at a saturation ceiling. Therefore, increases in atmospheric temperature do not translate into increased evaporative loss, because the boundary layer is already humidity-saturated and cloud-shielded. The study suggest that the basin is currently in a state of dynamic equilibrium, that is, the marginal increase in total rainfall is being absorbed by the system's high drainage capacity without a corresponding shift in the frequency of catastrophic outlier events.

This study recommends that future infrastructure should focus on managing chronic saturation like soil stability and landslide prevention, rather than exclusively focusing on acute events such as flash floods. As neighboring regions potentially face increasing aridity, this basin's stationary water surplus will become a critical strategic asset for regional water-sharing and biodiversity preservation. **S**trict regulations against large-scale land-use changes should be enforced. To move beyond potential evaporation and understand actual evapotranspiration, this study further recommends the installation of Eddy Covariance tower array, to allow for the direct measurement of water-vapor and carbon-dioxide flux to confirm the mechanistic drivers of the observed stationarity.

References

Blum, A. G., P.J. Ferraro, S.A. Archfield and K.R. Ryberg. (2020). The path forward for stationarity: Integrating internal variability and climate change. Water Resources Research, 56(2).

Brunner, M. I., E. Gilleland, and A.W. Wood. (2023). Hydrologic non-stationarity and its implications for future water security. Nature Reviews Earth & Environment, 4(5), 312–326. https://doi.org/10.1038/s43017-023-00409-w

Chineke, T. C., Jagtap, S. S., & Nwofor, O. (2020). West African monsoon: Is the August break "breaking" in the eastern humid zone of Southern Nigeria? Climatic Change, 103, 555–570. https://doi.org/10.1007/s10584-009-9780-2

Gleeson, T., L. Wang-Erlandsson, M. Porkka, T. Egli, F. Jaramillo, D. Gerten, S. Zipper and J.S. Famiglietti. (2020). The water cycling of the Anthropocene. Hydrology and Earth System Sciences, 24(8), 3831–3852. https://doi.org/10.5194/hess-24-38312020

Greve, P. W. Lucht, S. Tramberend, Y. Wada and D. Gerten. (2021). Irrigation of biomass plantations may globally increase water stress more than climate change. In Nat Comms 12 (1), pp. 1–9.

Gudmundsson, L., J., H.X. Boulange, S.N. Gosling, M.G. Grillakis and N. Hanasaki. (2021). Globally observed trends in mean and extreme river flow attributed to anthropogenic climate change. Science, 371(6534), 1159-1162.

Han, J., J. Wang, J. Zhao, H. Huang, T. Ning, and Y. Wang. (2023). A review of the Budyko framework: From theory to practice. Journal of Hydrology, 625, 130085. https://doi.org/10.1016/j.jhydrol.2023.130085

Han, S., H. Hu, H, F. Tian, Y. Ma, and K. Ichi. (2020). Global analysis of the energy-limited and water-limited fractions of the hydrological cycle. Hydrology and Earth System Sciences, 24(5), 2751-2770.

IPCC (2023). Climate Change 2023: Synthesis Report. Contribution of Working Groups I, II and III to the Sixth Assessment Report of the Intergovernmental Panel on Climate Change.

McVicar, T. R., Roderick, M. L., Donohue, R. J., & Li, L. T. (2022). The 'Evaporation Paradox' revisited: Global trends and local drivers in a warming climate. Nature Reviews Earth & Environment, 3, 435–452. (Directly supports your finding of stable evaporation despite global warming).

Moussa, R. and J.P. Lhomme. (2023). A physical interpretation of the aridity index within the Budyko Framework. Hydrology and Earth System Sciences.

Nigerian Meteorological Agency (NiMet). (2025). 2025 Seasonal Climate Prediction (SCP). Nigerian Meteorological Agency.

Pokhrel, Y., F.Felfelani, Y. Satoh, J. Boulange, P. Burek, N. Hanasaki, J. Schewe, H. Schmied, T. Stacke, T. Trautmann, and Y. Wada. (2021). Global terrestrial water storage and drought severity under climate change. Nature Climate Change, 11(3), 226–233. https://doi.org/10.1038/s41558-020-00972-w

Serinaldi, F. and C.G. Kilsby. (2021). Stationarity is dead, long live stationarity: The importance of historical baselines for risk assessment. Journal of Hydrology, 595, 126013.

Wang, J., F. Sun, W.H. Lim, H. Wang, W. Liu and C. Liu. (2022). Decoupled trends of evaporation and precipitation in high-latitude humid basins. Journal of Climate, 35(12), 3711-3727.